Biochimica et Biophysica Acta 1848 (2015) 2163–2171

Contents lists available at ScienceDirect

Biochimica et Biophysica Acta

journal homepage: www.elsevier.com/locate/bbamem

Interfacial stabilization of the antitumoral drug Paclitaxel in monolayers of GM1 and GD1a gangliosides

Valeria Heredia [a], Bruno Maggio [b], Dante M. Beltramo [a,c], Fernando G. Dupuy [d,*]

[a] Centro de Excelencia en Productos y Procesos de Córdoba (CEPROCOR), Argentina
[b] Centro de Investigaciones en Química Biológica de Córdoba (CIQUIBIC), UNC-CONICET, Departamento de Química Biológica, Facultad de Ciencias Químicas, Universidad Nacional de Córdoba, Argentina
[c] Consejo Nacional de Investigaciones Científicas y Tecnológicas (CONICET), Argentina
[d] Instituto Superior de Investigaciones Biológicas (INSIBIO), CONICET-UNT, and Instituto de Química Biológica "Dr. Bernabé Bloj", Facultad de Bioquímica, Química y Farmacia, UNT. Chacabuco 461, T4000ILI – San Miguel de Tucumán, Argentina

ARTICLE INFO

Article history:
Received 5 January 2015
Received in revised form 23 June 2015
Accepted 24 June 2015
Available online 26 June 2015

Keywords:
Antitumoral drug
Ganglioside
Favorable interactions
Interfacial stabilization
Monolayer
Micelle

ABSTRACT

Molecular interactions between the anti-cancer agent Paclitaxel (Ptx), and two gangliosides with different sialic acid content, GM1 and GD1a, were investigated using the Langmuir film balance technique. Ptx showed interfacial activity reducing the air/water surface tension by 18 $mN \cdot m^{-1}$. However, the drug was able to insert into preformed ganglioside monolayers at much higher surface pressures, indicating a preferential interaction of Ptx with GM1 and GD1a. Compression isotherms of binary mixtures of Ptx and GM1 or GD1a also indicated non-ideal mixed monolayers in which the drug became stabilized at the interface in the presence of gangliosides. Ptx reached much higher surface pressure values in the mixed monolayers than those sustained in pure Ptx, although partial desorption of the drug from the interface into the subphase was also observed at high Ptx contents. The mean molecular area of the mixtures showed condensation, mainly in the case of GD1a, whereas Ptx induced a decrease in the compressibility of monolayers when mixed with either GM1 or GD1a. Additionally, Brewster angle microscopy analysis indicated that higher amounts of Ptx are present at the mixed ganglioside/Ptx interface when compared to pure drug monolayers. Finally, GD1a micelles increased in size in the presence of Ptx, whereas GM1 micelles kept their diameter, according to dynamic light scattering measurements, which could be explained by the different properties of ganglioside monolayers. The results obtained on ganglioside–Ptx interactions allowed interpreting the different Ptx loading capacity of GM1 and GD1a, enabling them to act as potential drug carriers.

1. Introduction

Paclitaxel (Ptx), a natural product isolated from the Pacific yew tree *Taxus brevifolia*, is one of the most active anticancer agents used [1,2]. Nevertheless, due to its low aqueous solubility (less than 1 $\mu g \cdot mL^{-1}$) it causes difficulties in drug formulation [3,4]. Taxol® (Bristol-Myers Squibb, Princeton, NJ), one of the currently marketed formulations of Ptx, is usually prepared in 50% (v/v) polyoxyethylated castor oil (Cremophor EL®) and 50% dehydrated ethanol, a formulation that shows several toxicological, pharmacologic and pharmaceutical disadvantages [5,6]. Therefore, alternative formulations of Ptx are actively sought.

Recently, Leonhard et al. [7] described a novel system for aqueous delivery of Ptx consisting of self-assembled nanomicellar carriers of gangliosides, which allowed solubilizing as much as 6 $mg \cdot mL^{-1}$ of the drug. Gangliosides are complex glycosphingolipids formed by a common hydrophobic portion, the ceramide, and a polar head group composed of hexoses and sialosyl residues [8,9] that determine particular properties and aggregation structures of the molecule [10,11]. The incorporation of drugs into ganglioside micelles was shown to be spontaneous and the biological activities of this formulation showed no significant differences from the drug in free form [7]. Moreover, the efficiency of gangliosides on drug loading was highly dependent on the type of structure formed, i.e. micelle or liposome, a consequence of the ganglioside monomer shape and the molecular critical packing parameter [11]. In effect, the potential cargo capability significantly decreased in gangliosides such as GM3, forming large cylindrical micelles and even small vesicles, when compared to GM2 and GM1 [7], and which are able to form only micelles in aqueous solution [10–12].

Abbreviations: GM1, β-Gal-(1–3)-β-GalNAc-(1–4)-[α-Neu5Ac-(2–3)]-β-Gal-(1–4)-β-Glc-(1-1′)-N-Cer; GD1a, α-Neu5Ac-(2–3)-β-Gal-(1–3)-β-GalNAc-(1–4)-[α-Neu5A-(2–3)1-β-Gal-(1–4)]-β-Glc-(1–1)-Cer; HPTLC, high performance thin layer chromatography; PTFE, polytetrafluoroethylene (Teflon).

* Corresponding author at: Instituto Superior de Investigaciones Biológicas (INSIBIO), CONICET-UNT, and Instituto de Química Biológica "Dr. Bernabé Bloj", Facultad de Bioquímica, Química y Farmacia, UNT. Chacabuco 461, T4000ILI – San Miguel de Tucumán, Argentina.
E-mail address: fdupuy@fbqf.unt.edu.ar (F.G. Dupuy).

http://dx.doi.org/10.1016/j.bbamem.2015.06.022
0005-2736/

Although molecular interactions between Ptx and gangliosides are likely to play an important role in these differences, they have not been investigated so far in depth. Such information could have decisive influence on the partitioning, orientation, and conformation of the drug within the lipid micelle. Obtaining information on Paclitaxel–ganglioside interaction may thus provide useful insights that allow improving the design of new optimal drug delivery systems [13–15]. Being gangliosides natural, unmodified lipid molecules, delivery carriers based on ganglioside micelles would also avoid immune response against the vehicle and the drug, indicating that they can be considered as a suitable alternative for overcoming the low solubility of Ptx in biological media.

Within the scope described above, we studied miscibility and molecular interactions of paclitaxel with GM1 and GD1a in monolayers at the air/water interface. The stability and mixing behavior of Ptx/ganglioside in films at various molar ratios were analyzed by measuring mean molecular area, surface (dipole) potential and surface topography by Brewster angle microscopy. The effect of Ptx on the Gibbs elasticity of the mixed monolayers was also assessed in terms of surface compressional modulus and compared to that of pure components. The results indicate that although Ptx shows a relatively low surface activity, favorable interactions were found between the antineoplasic drug and the gangliosides, leading to an increased stabilization of Ptx at the interface. Variation of the monolayer surface pressure induced reversible release and uptake of the drug between the surface and the subphase of the mixed films, highlighting that Ptx-ganglioside interactions could be advantageous for a cargo system in which both uptake and release of the drug from the carrier is desirable. A higher loading capacity of GD1a micelles could also be inferred when compared to GM1, as the former shows an increased liquid expanded state and a more flexible geometrical constrain, which allow these micelles undergoing a larger increases in size upon drug binding.

2. Material and methods

2.1. Materials

Ptx was obtained from Yunnan Smandbet Co. Ltd. (Kunming, China) and stock solutions were prepared by dissolving the drug in ethanol. GM1 and GD1a gangliosides were purified by means of size exclusion chromatography from an extract of bovine brain gangliosides, a gift from Dr. Pablo Rodriguez. HPTLC of purified gangliosides in an amount at least 10 times that required for detection showed no contaminant spots after charring the plate with 50% (v/v) H_2SO_4. Stock solutions of gangliosides were prepared by dispersing them in bidistilled water at a final concentration of 7 mM, and then in chloroform:methanol:water (2:1:0.15, v/v). The subphase solution used for Langmuir monolayer experiments was 145 mM NaCl (Merck), prepared with water obtained from successive treatment in Elix 10 and Gradient A10 (Millipore) systems.

2.2. Langmuir film balance experiments

Ptx adsorption at the air–water interface or ganglioside monolayers were carried out in a small custom-made PTFE trough (15 mL) and under magnetic stirring in order to ensure uniform equilibration of concentration in the subphase. Compression isotherms were carried out in a KSV-Minitrough system (KSV-NIMA, Biolin Scientific) equipped with a 266 cm^2 PTFE trough and isometric compression by means of two hydrophilic movable barriers (Delrin). Surface pressure and surface potential of the film were simultaneously measured by means of Pt-plate and an air-ionizing ^{241}Am electrode located 5 mm above the surface and a Ag/AgCl miniature (Cypress System) as a reference electrode in the subphase, or with a vibrating plate surface potential meter (SPOT, KSV-NIMA), respectively. The whole system was enclosed in an acrylic box surrounded by a metallic grid connected to ground, in order to reduce external interference in the measurements of surface potential. Films were compressed at 3 $Å^2 \cdot molecule^{-1} \cdot min^{-1}$; two-fold reduction of the compression rate did not cause changes in isotherms. Temperature was maintained at 24 ± 0.5 °C by means of an external circulating water bath (Haake F3C) and a temperature sensor in the trough. Values are the average of three independent experiments.

2.3. Analysis of the isotherms

The surface compressional modulus (in-plane elasticity, C_S^{-1}) was calculated directly from the surface pressure-mean molecular area isotherms according to:

$$C_s^{-1} = -A\left(\frac{\partial \pi}{\partial A}\right)$$

where π is the surface pressure and A is the mean molecular area at the surface pressure π [16,17].

In-plane elasticity of Ptx/ganglioside mixtures was compared with the calculated mean elasticity of ideally mixed films, taking into account the Cs^{-1} of pure components, mean molecular area A_1 and A_2 and the mole fraction X_1 and X_2 of components 1 and 2, respectively, at the corresponding π [16], according to:

$$C_{s\pi}^{-1} = \left[X_1\left(\frac{A_1}{C_{s1}^{-1}}\right)_\pi + X_2\left(\frac{A_2}{C_{s2}^{-2}}\right)_\pi\right]^{-1} \cdot (X_1A_1 + X_2A_2).$$

Surface potential per unit of molecular surface density ($\delta V \cdot n^{-1}$), where n is the number of molecules per cm^2, was calculated from the surface (dipole) potential measured for the films (ΔV) and the mean molecular area A [18] at the surface pressure π:

$$\frac{\partial V}{n} = \Delta V \cdot A.$$

The mean molecular area and $\delta V \cdot n^{-1}$ of the mixtures at the corresponding surface pressure π were compared with the values predicted from the additivity rule [17] according to:

$$A_\pi = X_1(A_1)_\pi + X_2(A_2)_\pi$$

$$\frac{\delta V}{n_\pi} = X_1\left(\frac{\delta V}{n_1}\right)_\pi + X_2\left(\frac{\delta V}{n_2}\right)_\pi$$

where A_1, A_2 and $\delta V \cdot n_1^{-1}$, $\delta V \cdot n_2^{-1}$ are the mean molecular area and mean surface potential per unit of molecular surface density of component 1 and 2, respectively, at the surface pressure π [17].

Excess free energy of mixing (ΔG_m^E) was calculated from the integral of π–A curves of pure components and mixtures [17], between 1 and 7 $mN \cdot m^{-1}$, according to the formula:

$$\Delta G_m^E = \int_1^7 A_{1,2} \cdot d\pi - \left(X_1\int_1^7 A_1 \cdot d\pi + X_2\int_1^7 A_2 \cdot d\pi\right)$$

where A_1 and A_2 are the mean molecular area of components 1 and 2, respectively, and $A_{1,2}$ is the mean molecular area of the mixed film.

2.4. Brewster angle microscopy

Film imaging by Brewster angle microscopy (BAM) was performed with an auto-nulling imaging ellipsometer (Nanofilm EP3sw imaging ellipsometer, Accurion GmbH, Germany) equipped with a 532 nm laser, 20× objective, and CCD camera, operating at a resolution of 1 μm in the BAM mode. Quantitative reflectivity, which depends on the optical properties of the interface (thickness and refractive index) [19,20], was measured after calibration of the actual Brewster angle of

the subphase, by sensing the reflected p-polarized light at several angles of incidence. The public software ImageJ (1.43u Wayne Rasband, National Institutes of Health, Bethesda, MD) was used for gray level determination on the bare images obtained by BAM.

2.5. Dynamic light scattering

Average particle size of bulk aqueous dispersions of GM1 and GD1a gangliosides in 145 mM NaCl, at a 10 $mg \cdot mL^{-1}$ final concentration, was measured by dynamic light scattering (DLS) in the presence and in the absence of 1 $mg \cdot mL^{-1}$ Ptx, in a Delsa™ Nano Submicron Particle Size and Zeta Potential Particle Analyzer at a fixed scattering angle of 165°. Data were analyzed by Delsa Nano Beckman Coulter software (version 2.2) provided by manufacturer with CONTIN method. Measurements were carried out four times. Reported values are the mean ± standard error.

3. Results

3.1. Adsorption of Paclitaxel at the air–water interface

Adsorption of Ptx molecules at the aqueous interface was monitored by measuring the surface pressure π, which is the difference between the surface tension of the subphase, γ_0, and the surface tension, γ, after the injection of Ptx in the subphase. A maximum surface pressure value of ~18 $mN \cdot m^{-1}$ was obtained when the drug reached a concentration of more than 30 μM in the subphase (Fig. 1A), indicating the surface activity of the drug. Similar results have been reported for Docetaxel [14] in which 20 μM of the drug produced a maximum decrease in surface tension of 16 $mN \cdot m^{-1}$ with a calculated area per molecule at a saturated interface of 97.3 $Å^2 \cdot molec^{-1}$ according to the Gibbs isotherm. In comparison, following the same procedure, we found that the area occupied by Ptx after adsorption at interface was 126.8 $Å^2 \cdot molec^{-1}$.

Moreover, Ptx increased the surface potential when compared to the clean interface, although the maximal effect in ΔV was obtained at a Ptx-subphase concentration lower than that required for a maximum Δπ (Fig. 1A), showing the usually higher sensitivity of ΔV to detect molecular adsorption to the interface.

3.2. Insertion of Paclitaxel in ganglioside monolayers

Adsorption of Ptx at 10 μM final concentration in the subphase into preformed GM1 and GD1a monolayers at the air–water interface was investigated at several initial surface pressures (π_i) of films of either GM1 or GD1a. The interaction between Ptx and ganglioside monolayers increased surface pressure (Δπ), as seen in Fig. 1B, where Δπ is plotted as a function of π_i. This considerable increase indicates that Ptx was incorporated into monolayers made of either GM1 or GD1a ganglioside and even reached surface pressures ($\pi_i + \Delta\pi$) higher than 18 $mN \cdot m^{-1}$, the maximum surface pressure attained by Ptx alone in clean air/water interfaces. Indeed, the exclusion surface pressure, determined by the intersection of the extrapolated line of Δπ values to the abscissa axis (when adsorption of no Ptx molecules in monolayer occur, $\Delta\pi \approx 0$ $mN \cdot m^{-1}$) was 53.9 $mN \cdot m^{-1}$ in GM1 monolayers and 41.8 $mN \cdot m^{-1}$ in GD1a films (Fig. 1B, open and closed symbols, respectively). Thus, for both gangliosides, the exclusion surface pressure of Ptx occurred at surface pressures higher than the equilibrium surface pressure of Ptx alone, indicating that interfacial stabilization of the drug was induced by interaction with the lipids.

3.3. π–A isotherms of pure components

The π–A isotherms of pure GM1 and GD1a are similar to those reported in the literature (Fig. 2A), with a collapse point at 54.2 ± 1.9 $mN \cdot m^{-1}$ and 49.9 ± 3.4 $mN \cdot m^{-1}$ and limiting mean molecular area of 44.1 ± 1.8 $Å^2 \cdot molec^{-1}$ and 56.3 ± 5.7 $Å^2 \cdot molec^{-1}$, respectively [21–24]. The larger A values of GD1a reflect the bulkier and more negatively charged head group compared to that of GM1. Isotherms of GM1 and GD1a also show a slight change in slope between 20 and 25 $mN \cdot m^{-1}$ (Fig. 2A), which is more easily detected by the change in the surface compressibility modulus in that range of surface pressure (Fig. 2B); this is produced by limited formation of lactone bonds in the oligosaccharide chain, according to the ganglioside purification method employed [25]. On the other hand, Ptx does not form stable monolayers. A poorly defined collapse pressure at 10 $mN.m^{-1}$ is observed (Fig. 2A), in agreement with previous reports [26–28]. Successive compression/expansion cycles shifted the surface pressure–area curves progressively towards lower area values, indicating loss of surface material from the interface (not shown).

The analysis of the surface elasticity of the pure components (Fig. 2B) indicated that gangliosides monolayers formed liquid expanded films with a surface compressibility modulus below 100 $mN \cdot m^{-1}$, whereas Ptx films were more expanded, with a surface compressibility modulus lower than 10 $mN \cdot m^{-1}$.

Values of $\delta V \cdot n^{-1}$ plotted vs A of pure (GM1, GD1a and Ptx) films are shown in Fig. 2C. Despite the presence of a large polar head group with charged chemical groups like sialic residues, $\delta V \cdot n^{-1}$ of ganglioside was low and showed very small changes (<0.3 $fV \cdot cm^2 \cdot molec^{-1}$) during film compression (Fig. 2C) as reported in earlier works [21,29,30]

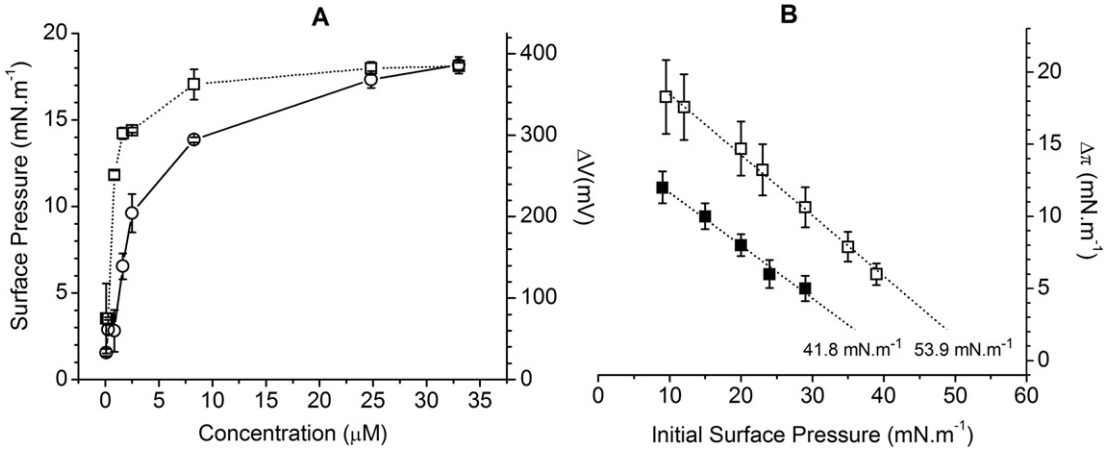

Fig. 1. A) Adsorption of Ptx at air–water interface at 24 °C. Surface pressure (circles) and surface (dipole) potential (squares) were simultaneously measured as a function of Ptx concentration in the subphase. B) Adsorption of Ptx and cut-off surface pressure in the presence of GM1 (open symbols) and GD1a (closed symbols) monolayers. Data are the mean of three independent experiments and were collected after 20 min of equilibration.

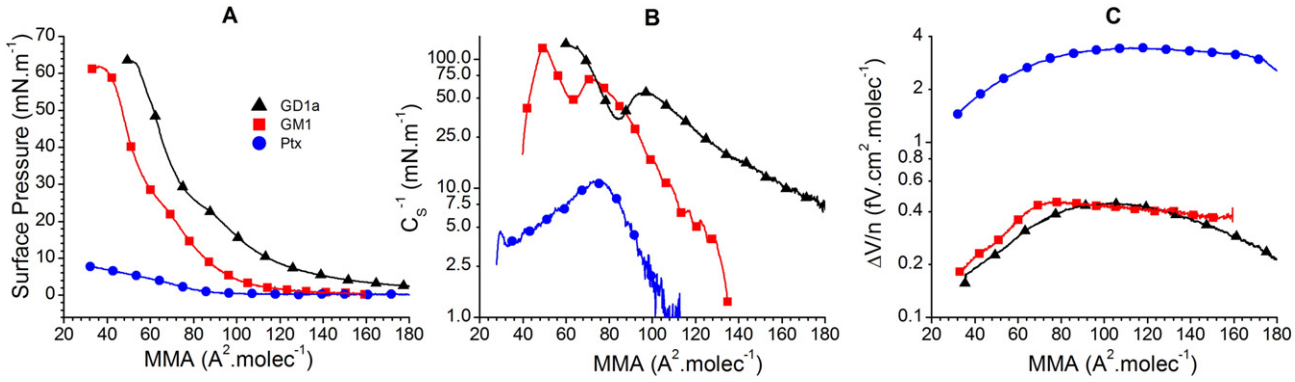

Fig. 2. Compression isotherms (A), surface compressibility modulus (B) and surface potential per unit of molecular surface density (C) as a function of the mean molecular area for GM1 (squares) and GD1a (triangles) gangliosides and Ptx (circles) films. Representative curves of three independent experiments are shown.

indicating rather low overall rearrangement of molecular dipole moment as a function of surface pressure.

On the other hand, the surface potential of Ptx films which, as far as we know, has not been previously reported, was characterized by high values of $\delta V \cdot n^{-1}$ between 2 and 3 $fV \cdot cm^2 \cdot molec^{-1}$ (Fig. 2C). Therefore, the interface of Ptx is considerably hyperpolarized compared to that of ganglioside monolayers.

3.4. Mixed monolayers of gangliosides and Paclitaxel

Representative compression isotherms of GM1/Ptx mixtures at several molar ratios are illustrated in Fig. 3A. The area per molecule of the lift-off of GM1/Ptx mixed monolayers decreased gradually upon increasing Ptx mole fraction (Fig. 3A). This was also observed in GD1a/Ptx mixed monolayers (Fig. 3B).

Mixed films of GM1 and Ptx formed stable monolayers at Ptx contents lower than 50%, which collapsed at surface pressures higher than the collapse surface pressure of pure components, suggesting a mixing-driven interfacial stabilization. However, higher Ptx content appears to induce loss of molecules from the interface. Indeed, even though gangliosides cannot probably be reduced more than about the minimum cross sectional area of two closely packed parallel hydrocarbon chains (30–40 $Å^2$) [29,31], mixed films with more than 50% of Ptx showed molecular area values much smaller than 40 $Å^2$ at high surface pressures (Fig. 3A, B).

In order to better ascertain this effect, we calculated the mean molecular area of the compression isotherms by considering only the GM1 molecules present in the film. In the inset of Fig. 3A, it can now be seen that no isotherms extends to area values smaller than 40 $Å^2$; in addition, at surface pressures higher than 30 $mN \cdot m^{-1}$, the compression curves of the mixtures are closely similar to that of pure GM1. However, at lower surface pressures, the isotherms became increasingly expanded, especially at a Ptx content higher than 50% (Fig. 3A, inset). In addition, when compression/expansion cycles were carried out at relatively high surface pressures, loss of molecules from the monolayer occurred (Fig. 4A), probably due to expulsion of Ptx molecules. Upon a second step of compression, π–A curves became more similar to those of pure gangliosides (Fig. 4A).

Compression isotherms of mixed GD1a/Ptx films essentially followed the same trend as that of GM1/Ptx system, with successive shift towards lower molecular area as Ptx content in the films was increased (Fig. 3B). The collapse surface pressure of 3:1 and 1:1 mixtures approached 70 $mN \cdot m^{-1}$, higher than the collapse of the individual components, suggesting not only good miscibility but also interfacial stabilization of the mixed film.

Molecular interactions of the components in the mixtures were analyzed by studying different mixing parameters as a function of the composition and by comparing them with the behavior of an ideal mixture. However, due to the low collapse surface pressure of Ptx, the analysis could be carried out only in the range of 0–7 $mN \cdot m^{-1}$.

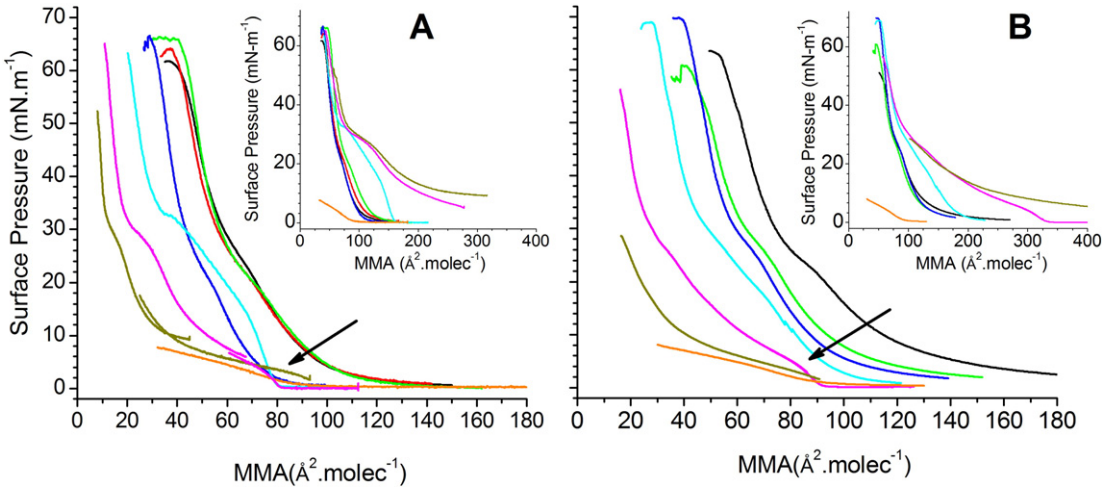

Fig. 3. Compression isotherms of GM1/Ptx (A) and GD1a/Ptx (B) mixtures at different compositions. The π–A curves shifted towards lower molecular areas upon increasing Ptx content; however, when mean molecular area values were calculated taking into account ganglioside molecules only (Insets), π–A curves in the high surface pressure region resembled those of pure GM1 (A) or GD1a (B) isotherms, respectively. Arrows indicate the presence of pure Ptx collapse point in mixtures with $X_{Ptx} > 0.5$. Mixture composition in ganglioside:Ptx molar ratio is: 1:0 (black lines), 12:1 (red), 6:1 (green), 3:1 (blue), 1:1 (cyan), 1:3 (magenta), 1:6 (dark yellow), 0:1 (orange).

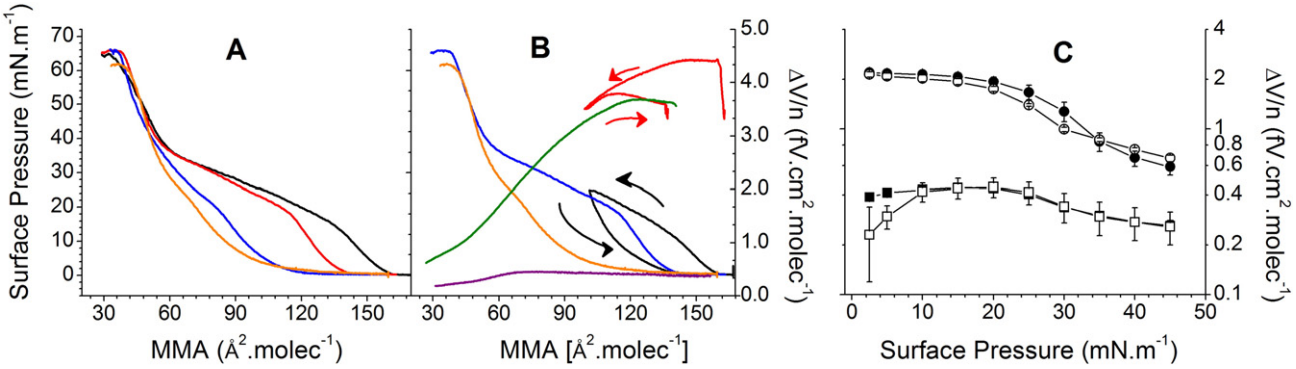

Fig. 4. Compression isotherms of 1:1 GM1:Ptx mixture. In (A), the full compression isotherm is depicted after a cycle of compression up to 10 (black line), 20 (red) and 30 (blue) $mN \cdot m^{-1}$ and expanding up to null surface pressure. GM1 compression isotherm is shown as an orange line. In (B), π–A curve (black line) and surface electrostatics (red line) for the whole compression/expansion cycle up to 20 $mN \cdot m^{-1}$ and the full compression afterwards (blue line) and its corresponding $\delta V \cdot n^{-1}$ (green line) are shown together with GM1 compression isotherm (orange line) and $\delta V \cdot n^{-1}$ (purple line) for comparison. In (C) $\delta V \cdot n^{-1}$ of 1:1 mixtures is plotted as a function of surface pressure for GM1:Ptx (closed circles) and GD1a:Ptx (open circles) mixed films and for pure GM1 (closed squares) and GD1a (open squares) films.

At 2.5 and 5 $mN \cdot m^{-1}$, the A values of GD1a/Ptx mixtures showed negative deviations of the mean molecular area over almost the entire range of compositions (Fig. 5A,D), indicating favorable interaction between the ganglioside and Ptx. On the other hand, GM1/Ptx mixed films at 5 $mN \cdot m^{-1}$ became expanded when compared to the additivity rule in films with Ptx contents higher than 50% (Fig. 5D), whereas at lower X_{Ptx}, mixed films were slightly condensed (Fig. 5D). A significant condensation of the GM1/Ptx mixtures was observed only at 2.5 mN m^{-1} and at Ptx content of $0.3 < X_{Ptx} < 0.8$ (Fig. 5A), suggesting that Ptx interacted more favorably with GD1a than with GM1.

The excess free energy of mixing (ΔG^E_m), which provides information on whether a particular mixture is energetically favored as compared to the ideally mixed components [17,23] is negative for all GD1a/Ptx mixtures, whereas GM1/Ptx mixed monolayers showed negative and positive ΔG^E_m, depending on film composition (Table 1).

On the other hand, the surface compressional moduli of the mixed films at 2.5 (Fig. 5B) and 5 $mN \cdot m^{-1}$ (Fig. 5E) were considerably higher than the theoretically predicted value for the mixtures of Ptx with any of the gangliosides, especially in the case of the 1:1 mixture which showed six and two fold increments at 2.5 $mN \cdot m^{-1}$ for GM1 and GD1a mixtures, respectively (Fig. 5B). This reflects that the favorable interactions occurring with tighter packing of the molecules in the film lead to increased elasticity in mixed monolayers with both gangliosides, being GM1/Ptx films stiffer than GD1a/Ptx ones.

Surface electrostatics measurements revealed hyperpolarization of the mixed interfaces when compared to the ideal behavior at 2.5 (Fig. 5C) and 5 $mN \cdot m^{-1}$ (Fig. 5F), with a maximal positive deviation also in the 1:1 mixtures composed of either GM1 or GD1a with Ptx (Fig. 5C,F), indicating dipole rearrangements induced by Ptx in the mixed films.

The equimolar (1:1) mixture of ganglioside/Ptx showed the highest deviations of the mixing molecular parameters, thus appearing as a defined threshold for interfacial drug solubilization (Fig. 5). Higher amounts of Ptx in the mixture leads to the excess of the drug being unmixed and phase separated, as indicated by the presence of the collapse

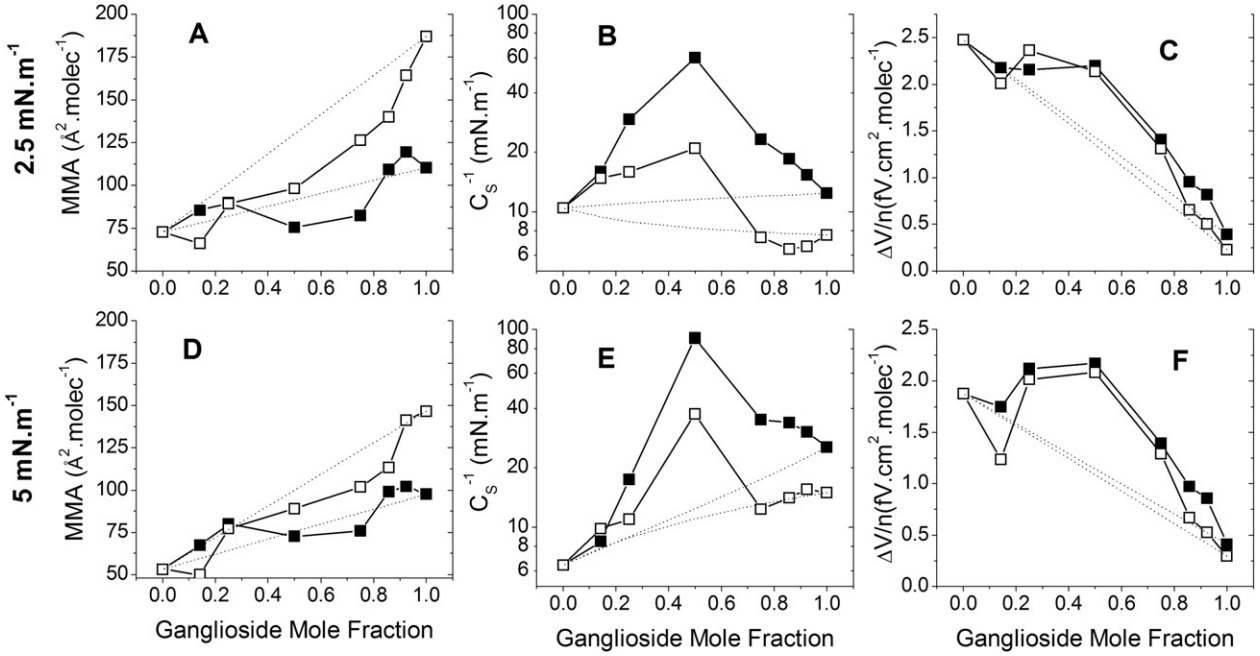

Fig. 5. Mixing parameters at 2.5 (A–C) and 5 (D–F) $mN \cdot m^{-1}$ of the mixture of Ptx with GM1 (closed symbols) and GD1a (open symbols) gangliosides. The mean molecular area (A, D), surface compressibility modulus (B, E) and surface potential per unit of molecular surface density (C, E) are plotted at different mixture compositions. Dotted lines are theoretically predicted values for ideal mixing behavior.

Table 1
Excess free energy of mixing of Ptx with GM1 and GD1a gangliosides in monolayers.

	ΔG^E_m (J·mol^{-1})		
Ganglioside:Ptx	6:1	1:1	1:6
GM1/Ptx	−202.0	−29.1	176.8
GD1a/Ptx	−1067.8	−607.1	−315.5

The excess free energy values of the mixtures at the indicated composition were calculated from the integral between 1 and 7 mN·m^{-1}of π–A isotherms.

point of pure Ptx during the compression of either GM1/Ptx mixed film or GD1a/Ptx (see arrows in Fig. 3B,C).

However, the equimolar ganglioside/Ptx mixtures showed molecular loss during compression, as discussed above (Fig. 3). The $\delta V \cdot n^{-1}$ values of 1:1 mixed films decreased upon compression at surface pressures higher than 20 mN·m^{-1} (Fig. 4C), which suggests that some drug molecules were squeezed out from the interface over that range of surface pressures, taking into account the much higher perpendicular molecular dipole of Ptx compared to gangliosides (Fig. 2C). Interestingly, partial recovery of Ptx molecules could be inferred when compression/expansion cycles were carried out: re-polarization of the interface occurred when film area was increased after compressing up to 20 mN·m^{-1} (Fig. 4B). Upon compression up to the collapse point, mixed films were also still hyperpolarized at 40 mN·m^{-1} when compared to pure ganglioside monolayer (Fig. 4B,C). This indicates that Ptx can remain in the mixed film at surface pressure values much higher than those that it can sustain in pure Ptx monolayers, probably due to favorable Ptx-ganglioside interactions that stabilize the drug at the interface.

3.5. Brewster angle microscopy

Film topography of GM1 [30] and GD1a (Fig. S1) monolayers studied by BAM typically shows a homogeneous surface and a steady increase in the reflected p-polarized light from null up to 5.0×10^{-6} upon film compression from 0 mN·m^{-1} up to the collapse point (Fig. 6A). Ptx films, on the other hand, exhibited values of p-reflectivity lower than those of ganglioside monolayers, with maximum reflectivity of 0.5×10^{-6} (Fig. 6A), but showing also homogeneous surface over the entire range of surface pressures of the isotherm (Fig. S1).

Mixed monolayers of ganglioside/Ptx at Ptx content lower than 50% showed homogeneous surfaces by BAM (not shown), but with increased reflectivity levels when compared to pure components at 5 mN·m^{-1} (Fig. 6B). However, at a Ptx content higher than $X_{Ptx} > 0.5$, the surface appearance of the mixtures with either GM1 or GD1a became complex (Fig. 7), with the presence of bright needle-like shaped domains within surface pressures ranging from 0 to 30 mN·m^{-1} in the case of GM1 (Fig. 7A) and at 5–20 mN·m^{-1} for GD1a mixtures (Fig. 7F). At higher surface pressures, two areas of different reflectivity levels could still be observed up to the collapse of the films (Fig. 7C,D and G,H). It has been previously shown that in bulk saturated solution, Ptx formed needle-like aggregates [6,32], suggesting that the domains formed in mixed ganglioside/Ptx films would result from Ptx accumulation at the interface due to favorable partition of Ptx molecules towards ganglioside films.

Interestingly, the reflectivity of the mixtures was higher than that of the films of both gangliosides and Ptx at 5 mN·m^{-1} (Fig. 6B), specially in the case of GD1a mixtures, suggesting an optical thickening of the interface (including possible variations of the refractive index) of the mixed film. Taking into account that hyperpolarization of the surface is also observed, Ptx would induce dehydration of the polar head group of gangliosides, reducing cancelation of interfacial dipole moments by water molecules [33,34]. If we consider the decreased reflectivity of the GD1a monolayer compared to that of GM1, the higher reflectivity values observed for mixed films composed of GD1a/Ptx 1:1 when compared to those of GM1/Ptx 1:1 (Fig. 6A,B) suggests that GD1a interfaces are able to accommodate higher amounts of Ptx than those of GM1.

3.6. Dynamic light scattering

According to monolayer experiments, a preferential interaction of Ptx with GD1a over GM1 could be inferred. Thus, we decided to study the average size of the micelles formed by either ganglioside in the presence and in the absence of the drug. DLS measurements indicated that the bulkier head group ganglioside GD1a formed smaller micelles than those of GM1, with diameters equal to 9.2 ± 1.1 and 12.8 ± 1.0 nm, respectively (Fig. 8, black lines) and in agreement with previous works [11,35]. Interestingly, upon Ptx interaction, GD1a micelles were able to enlarge up to 12.6 ± 0.9 nm (Fig. 8A), whereas the size of GM1 micelles remained almost unchanged (Fig. 8B), suggesting that GD1a micelles could load higher amounts of Ptx than those of GM1 ones.

4. Discussion

Recently, ganglioside micelles have proven to be a suitable option for delivery of hydrophobic antineoplasic taxanes, as their spontaneously Ptx loading and cellular uptake of the drug are not impaired when co-incubated with the lipids [7,36]. Also, in contrast with the current commercial formulation Taxol, ganglioside–Ptx formulations do not

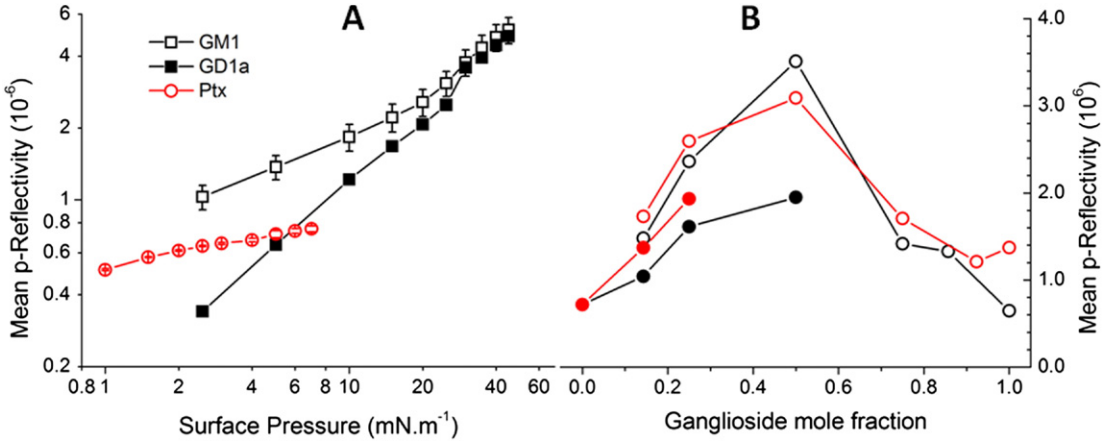

Fig. 6. p-Reflectivity of pure Ptx, GM1 and GD1a films as a function of surface pressure (A) determined by Brewster angle microscopy. (B) Mixed film p-reflectivity at 5 mN·m^{-1} of GM1:Ptx (red lines) and GD1a:Ptx (black lines) at different compositions was determined for the brighter phase (open symbols) and the darker phase (closed symbols) observed in the pictures of the mixtures.

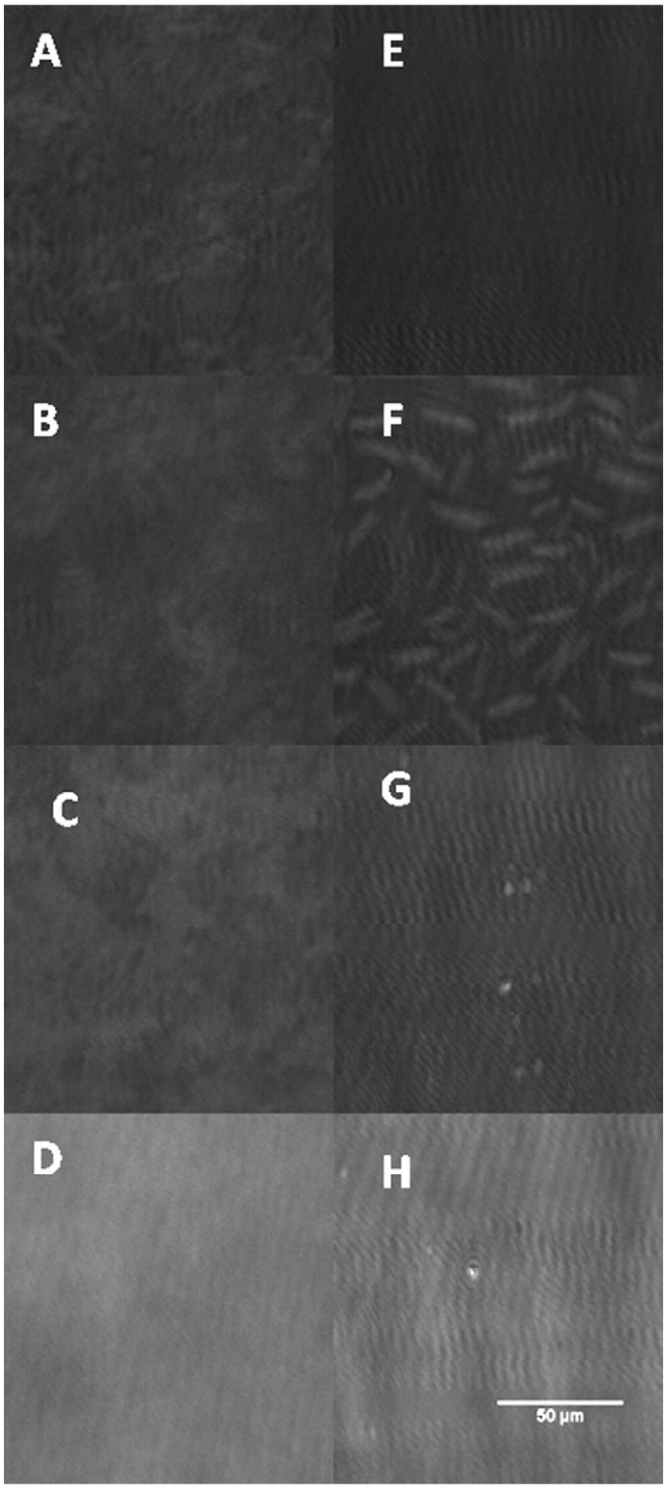

Fig. 7. BAM pictures of films taken at 20× magnification of the 1:1 mixtures of GM1:Ptx (A–D) and GD1a:Ptx (E–H) at 3.5 (A, E), 7.3 (B, F), 20 (C, G) and 53 (D, H) $mN \cdot m^{-1}$ during monolayer compression. White bar correspond to 50 μm.

need either ethanol or polyoxyethylated castor oil (Cremophor EL®), which has been indicated to be implicated in hypersensitivity syndrome [6]. On this regard, immune response against ganglioside based drug-carriers would not be expected, as they are natural lipid components of eukaryotic membranes. In-progress work suggests that the efficiency of gangliosides on drug loading depends on the type of structure formed: GD1a would be able to solubilize Ptx up to four times more than GM1 (unpublished results). Micelles were also shown to solubilize higher amounts of Ptx than vesicles, in gangliosides-based vehicles [7]. However, physicochemical data of Ptx and gangliosides and the understanding of the role that these molecular interactions may play in micelle formulation are still scarce.

4.1. Paclitaxel shows relatively low surface activity but is readily stabilized in ganglioside films

By means of the monolayer technique, we demonstrated that the surface activity of the Ptx drug, in spite of its hydrophobicity, is relatively low and form unstable monolayers that collapse at low surface pressures (~10 $mN \cdot m^{-1}$), in agreement with previous studies [26–28]. However, Ptx presents an important affinity towards ganglioside interfaces leading to a decrease in surface tension significantly higher than that caused by the drug in clean air–water interfaces, as indicated by high cut-off surface pressures (53.9 and 41.8 $mN \cdot m^{-1}$, for GM1 and GD1a, respectively), compared to the maximal surface pressure of pure Ptx (around 18 $mN \cdot m^{-1}$) but at rather high concentrations in the subphase.

4.2. Paclitaxel and the GM1 and GD1a gangliosides interact favorably in mixed monolayers

Previous studies on membrane interaction of Ptx and Docetaxel, both antineoplasic taxane derivatives, have been carried out in monolayer systems but only with glycerophospholipids [14,26–28,37–39]. Mixed phosphatidycholine–Ptx monolayers showed a decrease in film stiffness and lateral area expansion [37] when compared to pure DPPC monolayers, suggesting repulsive forces between mixed components. By contrast, mixed monolayers of Ptx with either GM1 or GD1a gangliosides were stiffer and showed negative deviations of the lateral area, especially in the case of GD1a mixtures, both of which indicate favorable interactions between the components in the films. Moreover, the excess free energy of mixing Ptx and GD1a was negative in mixtures at all mole fractions and of higher magnitudes than mixtures of Ptx and GM1, which were negative only at $X_{Ptx} < 0.5$. Thus, more favorable interactions can be inferred in mixtures of GD1a/Ptx than in those of GM1/Ptx. Hence, the differential molecular interactions between Ptx and gangliosides compared to phosphatidylcholines would suggest gangliosides as better agents than phosphatidycholines for incorporating and eventually releasing the drug for this kind of insoluble drugs [3].

On the other hand, hyperpolarization and increased p-reflectivity of Ptx-ganglioside mixtures were observed when compared to pure components, which could be interpreted as reorganizations of the fundamental dipole components of the carbohydrate moiety of the polar head group of gangliosides (including variations of their considerable hydration shell) as a consequence of an interfacial localization of Ptx molecules. BAM measurements had been previously carried out in docetaxel monolayers mixed with PCs [14]. Although no quantitative analysis of the reflectivity was reported in that work, surface topography of DPPC films mixed with taxol showed almost no differences with those of control DPPC films, as opposed to ganglioside/Ptx systems, indicating that only a DPPC-enriched film remained upon compression, at high surface pressures [14]. By contrast, the increased reflectivity of ganglioside–Ptx mixed films indicated Ptx insertion and stabilization at the interface at surface pressures that are not possible to attain by the pure drug. The presence of needle-like aggregates of Ptx in mixed monolayer at $X_{Ptx} > 0.5$, even at low surface pressures and up to collapse, also indicates a high local concentration of Ptx that could be reached as a consequence of the presence of gangliosides inducing interfacial stabilization of the drug. This kind of aggregates is observed in bulk solutions at high Ptx concentrations [32]; yet, they are absent in films composed of pure Ptx. Thus, favorable interactions between Ptx and ganglioside molecules can induce increased local concentrations of the drug at the interface.

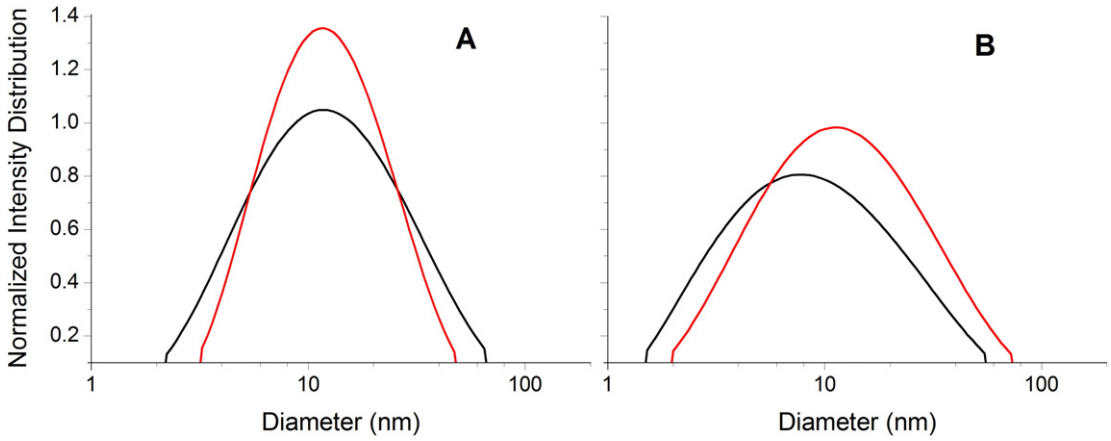

Fig. 8. Size distribution of GM1 (A) and GD1a (B) micelles in the absence (black lines) and presence (red line) of Ptx as determined by dynamic light scattering. Graphic is representative of four independent experiments.

Surface electrostatics of Ptx films and its mixtures, which has not been previously studied, proved to be a useful parameter for assaying the presence of taxol at the interface, as a consequence of the much higher polarization of Ptx films compared to those formed by gangliosides. By assaying the equimolar ganglioside:Ptx mixture we could corroborate the presence of Ptx associated to the interface of mixed monolayers at high surface pressure values (~40 $mN \cdot m^{-1}$),even though the shifting of the compression isotherms towards low area values indicated molecular loss from the interface. Actually, surface electrostatic measurements indicated partial and reversible expulsion of Ptx molecules from mixed films when the monolayer was compressed beyond the collapse surface pressure of Ptx. Interestingly, when surface pressure was decreased by expanding the films, the formerly expelled Ptx molecules could re-partition back into the ganglioside-containing interface, indicating that the equilibrium of the ganglioside–Ptx association can be reversibly modified by changing the surface pressure of the lipid interface. Partial desorption of Ptx from the interface of mixed monolayers of DSPC and Ptx at 24.5 °C was previously reported by Chou et al. [37], but the authors did not report reversibility of the desorption process. Since in a biological interface the lateral surface pressure can fluctuate by more than 20 $mN \cdot m^{-1}$ [40,41], a drug/lipid binding sensitive to surface pressure is a most important finding for a drug delivery system, in which a balance of favorable interaction between the cargo and the transporter and the rapid release of the drug are desirable. This kind of equilibrium could take place in bulk, when gangliosides form micelles.

4.3. Surface behavior of mixed ganglioside/Ptx monolayers correlates with micelle size

As previously shown, micelles formed by gangliosides would be better carriers as they solubilize higher amounts of taxanes than vesicles [7], the latter being the most common structures formed by phosphatidylcholines [42]. Correspondingly, we also gained several insights into monolayer experiments that indicate that GD1a could be a more appropriate drug-vehicle when compared to GM1. GD1a/Ptx mixed monolayers showed more negative values of ΔG_{ex} than those of GM1/Ptx, indicating more favorable molecular interactions in the former mixture.

In addition, micelles of GD1a, although smaller than those of GM1 when dispersed in bulk aqueous solution, increased its size in the presence of Ptx, whereas GM1 did not, as revealed by DLS, indicating a higher uptake of the drug by GD1a micelles. The smaller size of GD1a micelles is produced by geometrical constrains imposed by the bulkier and more negatively charged head group, compared with GM1, resulting in a lower packing parameter [43,44] $P = V/l.a_c$ and lower aggregation number for GD1a [11,12,35]. Taking into account that the ceramide moiety of GD1a and GM1 is essentially the same in both molecules, the hydrocarbon chains have to fill a larger lateral area in the micellar surface than that covered by the hydrocarbon chains of GM1; this corresponds to a smaller and more loosely packed micelles, of increased curvature, for GD1a micelles as compared to GM1. Interestingly, in monolayer experiments, the larger size of GD1a polar head group and the increased electrostatic repulsion of the two sialic residues, compared to GM1, also determine a more loosely packed interfacial region of GD1a, with more expanded compression isotherms and with lower elasticity. The more loosely packed interface of GD1a was able to accommodate more Ptx molecules than that of GM1, as indicated by quantitative analysis of BAM measurements and in agreement with results obtained in phosphatidylcholine/Ptx monolayers, in which more stable mixed films are formed by the more expanded DMPC than by the stiffer DSPC [39]. The thicker interface formed by GD1a/Ptx mixture compared to GM1/Ptx may be produced by head group reorientation towards the aqueous subphase [30], reduction of the lateral area occupied by the molecules at the interface and stretching of the hydrocarbon chains. The latter would also explain the stiffening of the films and the decrease of the compressibility modulus of mixed GD1a/Ptx monolayers by the enhancement of Van der Waals forces in the hydrocarbon region.

Thus, the present work indicates that the behavior of the drug in gangliosides monolayers can be used for characterizing molecular interactions related to potential nano-uptake/delivery applications. Although another targeting molecule would be necessary for directing the carrier system towards cancer cells, it should be noted that the high amounts of Ptx that gangliosides can solubilize and eventually transport did not produce macroscopic aggregation of Ptx, related to toxic side effects of the drug, such as complement activation [6], which can be observed with the commercial formulation based on castor oil and solvents.

5. Conclusions

GM1 and GD1a gangliosides favorably interact with the antineoplasic drug Paclitaxel in mixed monolayers, which allow achieving relatively high concentration of taxol at low surface pressures in lipid interfaces. The interaction showed to be reversible and highly dependent on the surface pressure of the interface, as equimolar ganglioside:Ptx mixtures composed of either GM1 or GD1a stabilized Ptx at surface pressures well above the one that the drug is able to reach alone; yet they were also able to allow release of Ptx upon film compression. The mixed Ptx/ganglioside monolayers in the case of GM1 and GD1a were stiffer and hyperpolarized when compared to the theoretically predicted values of ideal mixtures and in similar degree for both gangliosides.

However, GD1a/Ptx films showed negative deviation of the mean molecular area over a higher range of composition and surface pressure than that of GM1/Ptx mixtures, indicating a slight preferential interaction of Ptx with GD1a compared to GM1. GD1a systems would be able to load higher amounts of Ptx than GM1, as indicated by BAM measurements in monolayers. The differential cargo properties of the gangliosides could be ascribed to the looser packing of GD1a molecules in the micelles, compared to GM1.

Supplementary data to this article can be found online at http://dx.doi.org/10.1016/j.bbamem.2015.06.022.

Transparency document

The Transparency document associated with this article can be found, in the online version.

Acknowledgment

This work was supported by Consejo Nacional de Investigaciones Científicas y Técnicas (CONICET), (grant PIP 11220100100502), Agencia Nacional de Promoción Científica y Tecnológica (ANPCyT) (BID-PICT 1381) and Secretaría de Ciencia y Tecnología, Universidad Nacional de Córdoba (SeCyT, UNC) (C152/10). VH is a researcher from Centro de Excelencia en Productos y Procesos (CEPROCOR), Ministerio de Industria, Comercio, Minería y Desarrollo Científico Tecnológico, Provincia de Córdoba; and BM, DMB and FGD are researchers from CONICET.

References

[1] M.C. Wani, H.L. Taylor, M.E. Wall, P. Coggon, A.T. McPhail, J. Am. Chem. Soc. 93 (1971) 2325–2327.
[2] B.R. Goldspiel, Pharmacotherapy 17 (1997) 110S–125S.
[3] K.M. Huh, S.C. Lee, Y.W. Cho, J. Lee, J.H. Jeong, K. Park, J. Control. Release 101 (2005) 59–68.
[4] P. Crosasso, M. Ceruti, P. Brusa, S. Arpicco, F. Dosio, L. Cattel, J. Control. Release 63 (2000) 19–30.
[5] R.T. Liggins, W.L. Hunter, H.M. Burt, J. Pharm. Sci. 86 (1997) 1458–1463.
[6] J. Szebeni, C.R. Alving, S. Savay, Y. Barenholz, A. Priev, D. Danino, Y. Talmon, Int. Immunopharmacol. 1 (2001) 721–735.
[7] V. Leonhard, R.V. Alasino, I.D. Bianco, A.G. Garro, V. Heredia, D.M. Beltramo, J. Control. Release 162 (2012) 619–627.
[8] B. Maggio, G.A. Borioli, M. Del Boca, L. De Tullio, M.L. Fanani, R.G. Oliveira, C.M. Rosetti, N. Wilke, Cell Biochem. Biophys. 50 (2008) 79–109.
[9] S. Sonnino, L. Mauri, V. Chigorno, A. Prinetti, Glycobiology 17 (2007) 1R–13R.
[10] L. Cantu, E. Del Favero, P. Brocca, M. Corti, Adv. Colloid Interface Sci. 205 (2014) 177–186.
[11] B. Maggio, J. Albert, R.K. Yu, Biochim. Biophys. Acta 945 (1988) 145–160.
[12] B. Maggio, Biochim. Biophys. Acta 815 (1985) 245–258.
[13] C. Bourgaux, P. Couvreur, J. Control. Release 190 (2014) 127–138.
[14] A. Fernandez-Botello, F. Comelles, M.A. Alsina, P. Cea, F. Reig, J. Phys. Chem. B 112 (2008) 13834–13841.
[15] J.K. Seydel, E.A. Coats, H.P. Cordes, M. Wiese, Arch. Pharm. (Weinheim) 327 (1994) 601–610.
[16] S. Ali, J.M. Smaby, H.L. Brockman, R.E. Brown, Biochemistry 33 (1994) 2900–2906.
[17] G. Gaines, Insoluble Monolayers at Liquid–gas Interfaces, Interscience Publishers, New York, 1966.
[18] D.O. Shah, J. Colloid Interface Sci. 32 (1970) 577–583.
[19] C. Lheveder, J. Meunier, S. Hénon, Brewster angle microscopy, in: A. Baszkin, W. Norde (Eds.), Physical Chemistry of Biological Interfaces, Marcel Dekker Inc., New York, Basel 2000, pp. 559–576.
[20] D. Vollhardt, V.B. Fainerman, Adv. Colloid Interface Sci. 154 (2010) 1–19.
[21] D.C. Carrer, B. Maggio, Biochim. Biophys. Acta 1514 (2001) 87–99.
[22] S.L. Frey, E.Y. Chi, C. Arratia, J. Majewski, K. Kjaer, K.Y. Lee, Biophys. J. 94 (2008) 3047–3064.
[23] B. Maggio, Chem. Phys. Lipids 132 (2004) 209–224.
[24] B. Maggio, G.D. Fidelio, F.A. Cumar, R.K. Yu, Chem. Phys. Lipids 42 (1986) 49–63.
[25] G.D. Fidelio, T. Ariga, B. Maggio, J. Biochem. 110 (1991) 12–16.
[26] S.-S. Feng, K. Gong, J. Chew, Langmuir 18 (2002) 4061–4070.
[27] M.C. Giuffrida, F. Dosio, F. Castelli, M.G. Sarpietro, Int. J. Pharm. 475 (2014) 624–631.
[28] L. Zhao, S.S. Feng, M.L. Go, J. Pharm. Sci. 93 (2004) 86–98.
[29] B. Maggio, Prog. Biophys. Mol. Biol. 62 (1994) 55–117.
[30] C.M. Rosetti, R.G. Oliveira, B. Maggio, Langmuir 19 (2002) 377–384.
[31] D. Marsh, Handbook of Lipid Bilayers, Second ed. CRC Press, Taylor & Francis Group, 2013.
[32] S.V. Balasubramanian, R.M. Straubinger, Biochemistry 33 (1994) 8941–8947.
[33] A. Mashaghi, P. Partovi-Azar, T. Jadidi, N. Nafari, P. Maass, M.R. Tabar, M. Bonn, H.J. Bakker, J. Chem. Phys. 136 (2012) 114709.
[34] O.N. Oliveira Jr., D.M. Taylor, H. Morgan, Thin Solid Films 210-211 (Part 1) (1992) 76–78.
[35] L. Cantu, M. Corti, S. Sonnino, G. Tettamanti, Chem. Phys. Lipids 41 (1986) 315–328.
[36] V. Leonhard, R. Alasino, I.D. Bianco, D.M. Beltramo, Nanomedicine Nanotechnol. 4 (2013).
[37] T.-H. Chou, I.M. Chu, C.-H. Chang, Colloids Surf. B: Biointerfaces 25 (2002) 147–155.
[38] L. Zhao, S.S. Feng, J. Colloid Interface Sci. 300 (2006) 314–326.
[39] L. Zhao, S.S. Feng, J. Colloid Interface Sci. 274 (2004) 55–68.
[40] M.C. Phillips, D.E. Graham, H. Hauser, Nature 254 (1975) 154–156.
[41] S.-s. Feng, Langmuir 15 (1999) 998–1010.
[42] A. Sharma, R.M. Straubinger, Pharm. Res. 11 (1994) 889–896.
[43] P.R. Cullis, M.J. Hope, C.P. Tilcock, Chem. Phys. Lipids 40 (1986) 127–144.
[44] J.N. Israelachvili, S. Marcelja, R.G. Horn, Q. Rev. Biophys. 13 (1980) 121–200.